VIP Drug Discovery Very Important Paper

International Edition: DOI: 10.1002/anie.201607338
German Edition: DOI: 10.1002/ange.201607338

Natural-Product-Inspired Aminoepoxybenzoquinones Kill Members of the Gram-Negative Pathogen *Salmonella* by Attenuating Cellular Stress Response

Franziska A. Mandl[+], Volker C. Kirsch[+], Ilke Ugur, Elena Kunold, Jan Vomacka, Christian Fetzer, Sabine Schneider, Klaus Richter, Thilo M. Fuchs, Iris Antes, and Stephan A. Sieber**

Abstract: *Gram-negative bacteria represent a challenging task for antibacterial drug discovery owing to their impermeable cell membrane and restricted uptake of small molecules. We herein describe the synthesis of natural-product-derived epoxycyclohexenones and explore their antibiotic activity against several pathogenic bacteria. A compound with activity against Salmonella Typhimurium was identified, and the target enzymes were unraveled by quantitative chemical proteomics. Importantly, two protein hits were linked to bacterial stress response, and corresponding assays revealed an elevated susceptibility to reactive oxygen species upon compound treatment. The consolidated inhibition of these targets provides a rationale for antibacterial activity and highlights epoxycyclohexenones as natural product scaffolds with suitable properties for killing Gram-negative Salmonella.*

The increasing spread of multiresistant bacteria represents a fundamental threat to human health. While a few antibiotics of last resort are still effective against resistant Gram-positive bacteria, the most pressing problem stems from untreatable clinical Gram-negative isolates.[1] Here, the largely impermeable cell membrane impairs small-molecule uptake, which represents a major challenge for drug discovery.[2] For example, infections caused by resistant non-typhoidal *Salmonella* serotypes are of particular concern.[3] In the past, natural products such as β-lactams and aminoglycosides have been a rich source for antibiotic discovery, providing effective therapeutics in clinical use. However, the majority of natural-product antimicrobial drugs only address a limited scope of cellular targets, comprising cell wall, protein, and DNA biosynthesis. Thus, to get around resistance within these targets, searching for less explored natural product scaffolds and in-depth studies on their mechanism of action could provide additional and thus far unexploited cellular pathways suitable for drug development. Aminoepoxycyclohexenones (AECs) represent a prime example of such a privileged scaffold present in numerous natural products. They comprise the subclass of aminoepoxyhydroxycyclohexenones (AEHCs) with the amino functional group at either the 2′- (*ortho*, type I) or 5′-position (*meta*, type II), including LL-C10037α (**1**), asukamycin A1 (**2**), epoxyquinomycin C (**3**), and cetoniacytone A (**4**; Figure 1 A). Moreover, structural diversity is increased by the biosynthesis of related aminoepoxybenzoquinones (AEBQs, here referred to as type III) such as epoxyquinomycin B (**5**) and G-7063-2 (**6**; Figure 1 A). Interestingly, AEHCs as well as related AEBQs exhibit prevalidated activity against Gram-positive and even Gram-negative bacteria.[4] The presence of both an intact epoxide moiety and the Michael acceptor system is crucial for their antibacterial bioactivity, suggesting that alkylation of enzyme active sites could be a substantial part of the thus far uncharacterized cellular mechanism.[5] Herein, we exploited the antibiotic activity and cellular mechanism of structurally diverse aminoepoxycyclohexenones (I–III) by chemical, biochemical, and proteomic methods. Two compounds were identified that exhibit low micromolar activity against *S.* Typhimurium by addressing enzymes controlling oxidative stress. Moreover, the structure and mechanism of one target protein with unknown function were explored, giving unprecedented insight into the aminoepoxycyclohexenone mode of action.

To determine the bioactivities and cellular targets of aminoepoxycyclohexenones I–III, we synthesized a suite of molecules equipped with aliphatic and aromatic amide side chains and functionalized them with an alkyne tag (Figure 1 B). The alkyne tag served as a benign handle for target identification by Huisgen/Sharpless/Meldal cycloaddition (click chemistry, CC) to rhodamine or biotin azides.[6] Furthermore, corresponding benzoquinone probes lacking the crucial epoxide moiety were prepared as controls for cellular and proteomic studies. The syntheses of the probes were based on established procedures[7] and initiated by oxidative dearomatization of Boc-protected 2,5-dimethoxy-

[*] Dr. F. A. Mandl,[+] V. C. Kirsch,[+] E. Kunold, J. Vomacka, C. Fetzer, Dr. S. Schneider, Dr. K. Richter, Prof. Dr. S. A. Sieber
Center for Integrated Protein Science
Department Chemie, Technische Universität München
Lichtenbergstrasse 4, 85747 Garching (Germany)
E-mail: stephan.sieber@tum.de

Dr. I. Ugur, Prof. Dr. I. Antes
Center for Integrated Protein Science
Department für Biowissenschaften, Technische Universität München
Erlenmeyer-Forum 8, 85354 Freising (Germany)
E-mail: antes@tum.de

Prof. Dr. T. M. Fuchs
Lehrstuhl für Mikrobielle Ökologie
Zentralinstitut für Ernährungs- und Lebensmittelforschung
Technische Universität München
Weihenstephaner Berg 3, 85354 Freising (Germany)

[+] These authors contributed equally to this work.

Supporting information for this article can be found under: http://dx.doi.org/10.1002/anie.201607338.

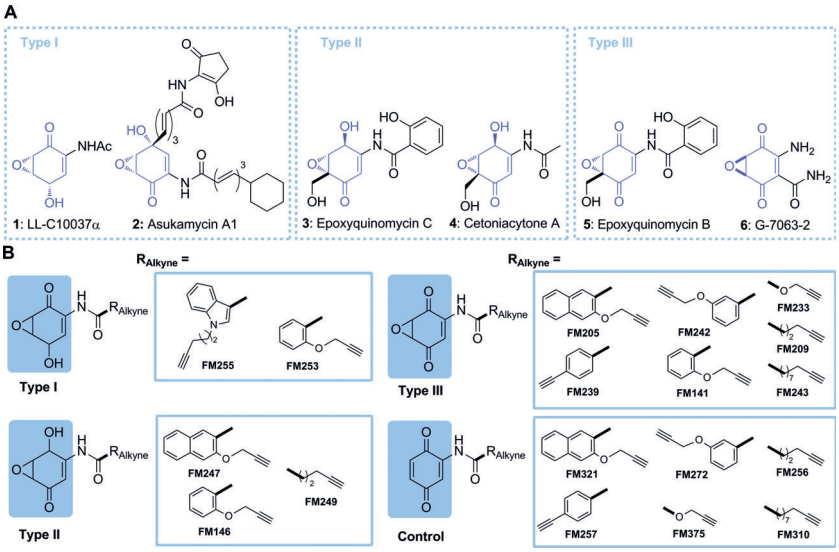

Figure 1. A) Representative aminoepoxycyclohexenone natural products: LL-C10037α (**1**), asukamycin A1 (**2**), epoxyquinomycin C (**3**), and cetoniacytone A (**4**) belong to the AEHC subclass (type I/II). Epoxyquinomycin B (**5**) and G-7063-2 (**6**) are members of the AEBQ subclass (type III).[4,8] B) Structures of diverse type I–III aminoepoxycyclohexenone ABPP probes and their corresponding epoxide-lacking benzoquinone controls.

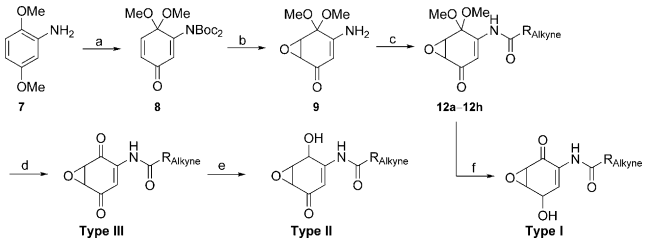

Scheme 1. Synthesis of type I and II AEHCs and type III AEBQs.[7] Reagents and conditions: a) 1. Boc_2O, THF, 70 °C, 16 h, 99%; 2. iodobenzene dipivalinate, MeOH, 0 °C→RT, 16 h, 84%; 3. Boc_2O, THF, 70 °C, 16 h, 68%; b) 1. H_2O_2, NaOH, THF, RT, 16 h, 53%; 2. trifluoroacetic acid, CH_2Cl_2, RT, 2 h, 96%; c) synthesized acids or acid chlorides **11a–11e**, lithium *tert*-butoxide, THF, −10 °C→RT, 4–16 h, 30–73%; d) $BF_3{\cdot}OEt_3$, CH_2Cl_2, −20 °C→RT, 14 h, 68–93%; e) $NaBH(OAc)_3$, MeOH, 0 °C→RT, 2 h, 53%; f) 1. $LiBHEt_3$, THF, −78 °C→RT, 3 h; 2. montmorillonite K10, CH_2Cl_2, RT, 16 h, 70% over two steps.

aniline (**7**) with iodobenzene dipivalinate (a; Scheme 1), followed by epoxidation using aqueous hydrogen peroxide solution and subsequent deprotection with trifluoroacetic acid (b). The Michael acceptor–epoxide key fragment **9** was further coupled to various alkyne-tagged acids or acid chlorides (see the Supporting Information, Section S9.1) by amide bond formation (c). Next, the acetal of the partially protected quinones (**12a–12h**) was removed with boron trifluoride diethyl etherate leading to type III AEBQs; subsequent reduction gave access to type II AEHCs. Upon inverting these two steps (d, e), type I AEHCs were generated (f). Benzoquinone analogues lacking the epoxide moiety (control, Figure 1B) served as reference compounds for phenotypic studies and labeling experiments (Scheme S1 and Table S1). Prior to proteomic target identification, all compounds were tested for the inhibition of bacterial growth against a panel of 16 different strains, including major pathogens such as *S. aureus*, multiresistant *S. aureus* (MRSA), and *S.* Typhimurium (Table S2).

Interestingly, type III AEBQs **FM205** and **FM243** as well as type I AEHC **FM255** inhibited the growth of Gram-positive strains, including MRSA, with minimal inhibitory concentrations (MICs) of 10 μM. Contrary, analogues of these compounds with an acetal group (**12a–12h**, Scheme 1) did not show growth inhibition (up to 300 μM), suggesting that the carbonyl or reduced hydroxy moieties are essential for the antibiotic activity. Strikingly, AEBQs **FM233** and **FM239** inhibited the growth of *S.* Typhimurium LT2 and TA100 and *S. enteritidis* with MICs of about 30 μM while the corresponding controls lacking the epoxide (Figure 1B and Scheme S1) did not affect viability. Satisfyingly, **FM233** displayed only low toxicity (< 15% apoptotic cells) in apoptosis assays against A549 cells at concentrations up to 150 μM (Figure S1). However, as the metabolic activity was impaired in human cells (Figure S2 and Table S3), we utilized a more complex and representative model of toxicity evaluation based on a whole organism. The nematode *Caenorhabditis elegans*[9] tolerated high doses of **FM233** as well as the inactive control **FM375** (highest tested concentration: 500 μM) over a period of five days without any signs of toxicity or developmental defects. Moreover, normal production of L1 larvae and eggs was observed whereas doxorubicin (100 μM), a toxic control, led to growth arrest (Figure S3). Contrary to extensive investigations of AEHC and AEBQ targets in human cells, the bacterial mode of action of this compound class has remained elusive.[10] Thus we applied our probe molecules in activity-based protein profiling (ABPP)[11] experiments and incubated several Gram-positive and Gram-negative strains with probe molecules in situ. The cells were lyzed, the probe-tagged proteins were clicked to rhodamine azide and separated by SDS-PAGE, and labeled proteins were then visualized by fluorescence scanning (Figure 2A). Whereas all *S. aureus* strains exhibited largely comparable labeling patterns of discrete cytosolic protein bands (Figure S4), a closer inspection of the *Salmonella* specific targets revealed striking differences between the antibiotic AEBQs (**FM239** and **FM233**) and their corresponding inactive controls lacking the epoxide moiety (**FM257** and **FM375**; Figure S5). For example, **FM233** labeled several distinct proteins (e.g., a prominent band at 30 kDa) that are absent in the **FM375** treated sample, suggesting that the epoxide addresses targets essential for bacterial viability (Figure 2A, B). In contrast, these probes did not reveal pronounced labeling in *S. aureus* and exhibited no MIC, suggesting a species-specific mode of action (Figure S6). Owing to the challenging discovery of druggable targets especially in Gram-negative strains, we selected antibiotic

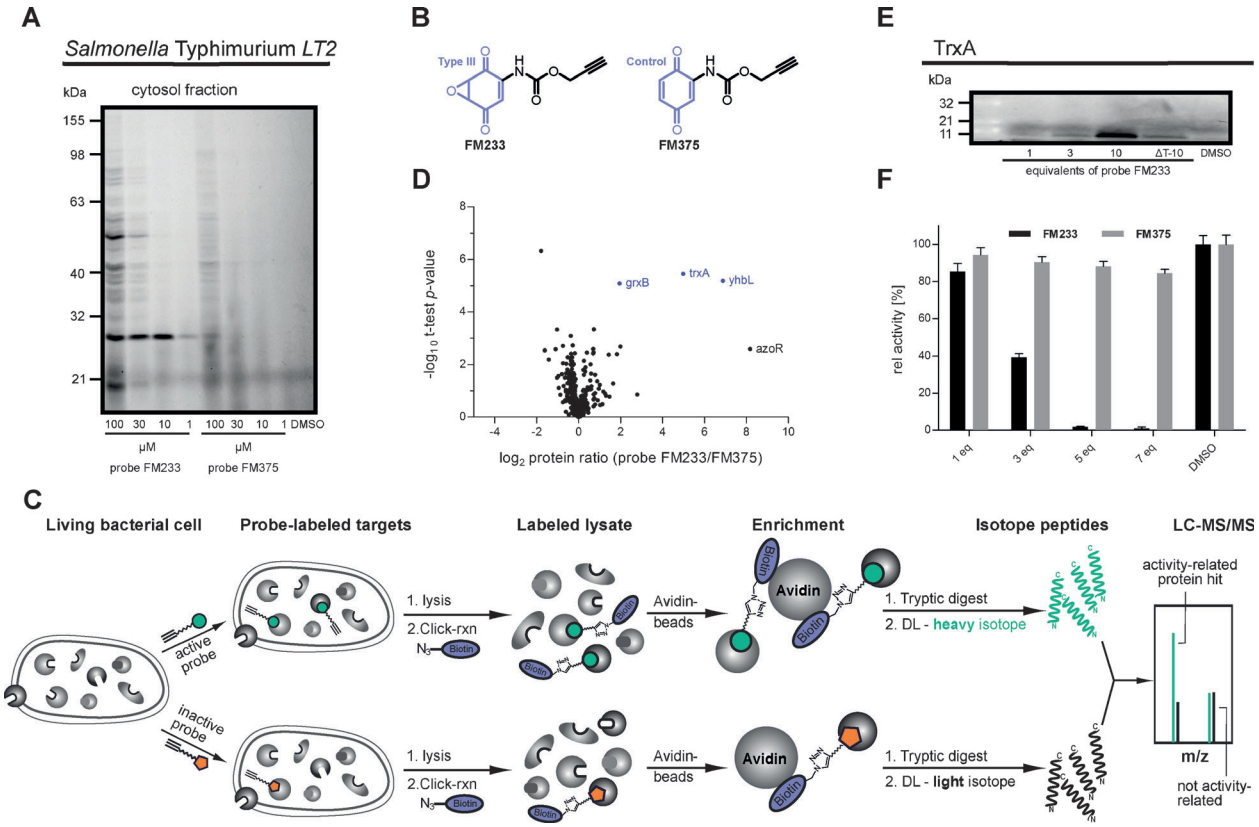

Figure 2. A) Fluorescence SDS gel of *S.* Typhimurium LT2 labeled in situ with the active probe **FM233** and the inactive control **FM375**. B) Structures of the probes used for labeling. C) Gel-free quantitative proteomics studies based on dimethyl labeling. D) Volcano plot of the enrichment analysis. Blue dots represent proteins that were significantly enriched at an FDR of 0.01 (Student's t-test, Benjamini–Hochberg truncation). E) Target validation by concentration-dependent labeling of recombinant TrxA. ΔT = heat-denatured TrxA labeled with 10 µM **FM233**. F) Inhibition of TrxA by **FM233** monitored in a turbidimetric assay of insulin disulfide reduction. Shown are two independent experiments, each performed in technical triplicate; error bars represent the standard deviation of the mean.

FM233 as a promising starting point for a detailed mechanism-of-action analysis in *S.* Typhimurium LT2.

For quantitative proteomic studies, cells were incubated with either active **FM233**, inactive **FM375**, or a DMSO control, lyzed, separated into soluble and insoluble fractions, and clicked to biotin azide. Afterwards, labeled proteins were enriched on avidin and digested by trypsin, and finally, the peptides were modified with either heavy or light isotopes by dimethyl labeling (DL, Figure 2C). Both samples were pooled and analyzed by liquid chromatography (LC) in combination with high-resolution mass spectrometry (MS). Proteins that were specifically bound by the probe revealed a high enrichment (criteria: $\log_2 \geq 2$ and statistically significant; Student's t-test, Benjamini–Hochberg FDR of 0.01) compared to those that are background binders and also present in the DMSO control (Figure S7). To focus only on target proteins that are associated with the antibiotic mode of action, we performed additional gel-free studies in comparison with the inactive control **FM375** (Figure 2D) and identified three significantly enriched targets in the soluble fraction: glutaredoxin 2 (GrxB), thioredoxin-1 (TrxA), and sigma cross-reacting protein 27A (SCRP-27A). Although not matching the significance criteria, it is worth noting that FMN-dependent azoreductase R (AzoR), a quinone reductase protecting the cell from thiol-specific stress caused by quinone electrophiles,[12] was discovered as well. When this experiment was carried out with the insoluble fraction, no significant hits were discovered. These results suggest that the molecule is cell-permeable and largely addresses cytosolic proteins (Figure S8). Furthermore, the characteristic cytosolic 30 kDa band could be assigned to be SCRP-27A by gel-based MS studies (Figure S9). Whereas GrxB and TrxA are associated with bacterial redox pathways, little is known about SCRP-27A.[13] To validate probe binding and to investigate the mechanism of inhibition, all targets were overexpressed, purified, and analyzed in various assay systems. Labeling studies with recombinant SCRP-27A, TrxA, and GrxB proteins and corresponding expression strains confirmed **FM233** binding whereas, in line with the proteome data, the **FM375** control probe was largely inactive (Figure 2E and Figures S10–S14).

SCRP-27A turned out to be most challenging as it is a protein of unknown function. It belongs to the DJ-1 protein superfamily[14] with a predicted Cys-His-Glu triad characteristic of glutamine amidotransferases, hydrolases, and proteases.[15] To gain insight into the mechanism, we first crystallized recombinant SCRP-27A and determined its X-ray structure to 1.75 Å resolution. (Figure 3A).[21] Interest-

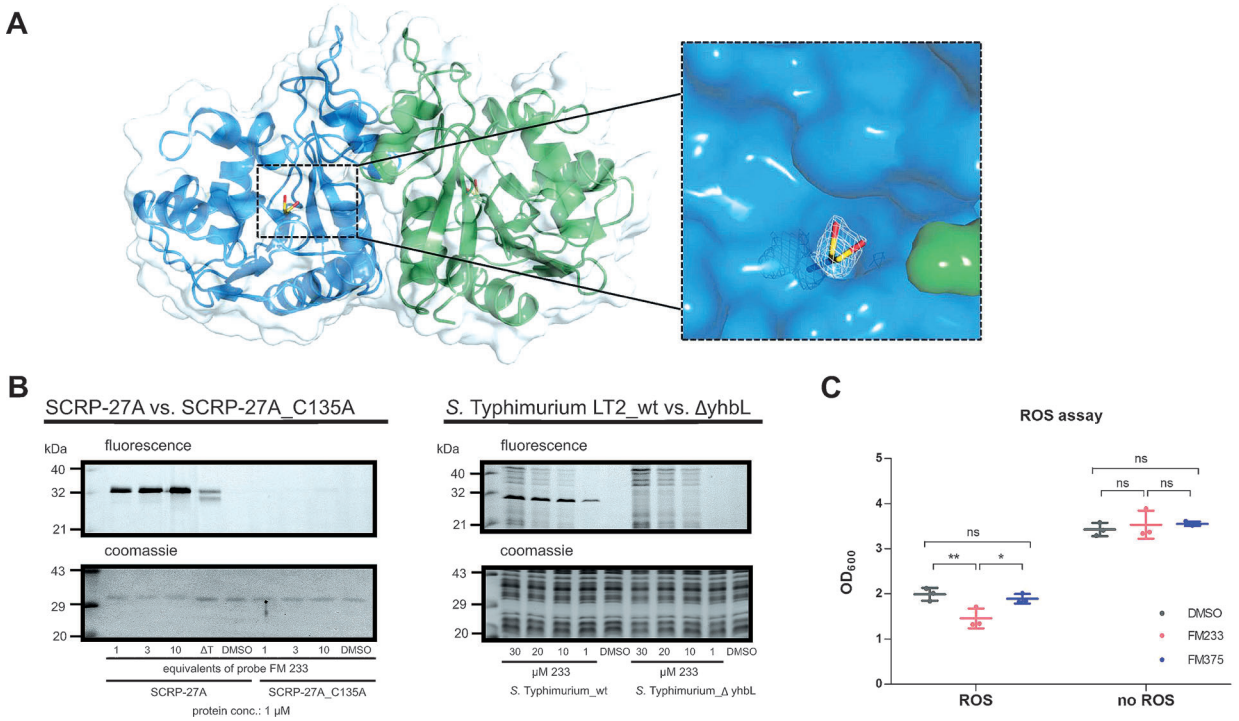

Figure 3. A) Crystal structure of *S.* Typhimurium SCRP-27A determined with a resolution of 1.75 Å.[21] The dimeric biomolecule (shown as a ribbon in green and blue) is overlaid with its semi-transparent surface and completed by the crystallographic symmetry. Enlarged image of the predicted active site: Cys135 is displayed as a stick model, with the corresponding F_o-F_c difference electron density contoured at 2σ (gray mesh). Cys135 adopts two alternative conformations and is most likely oxidized to sulfenic acid.[18] B) Concentration-dependent labeling of **FM233** in SCRP-27A and the SCRP-27A-C135A mutant (left) as well as in *S.* Typhimurium LT2 and LT2-Δ*yhbL* (right) confirmed the binding site of **FM233**. C) ROS assay with active **FM233** and inactive **FM375** at a concentration of 100 μM compared to the untreated control (no ROS). ns = not significant; *: $p<0.05$; **: $p<0.01$.

ingly, an exposed Cys135 residue located in a distinct pocket was observed, which is highly conserved among DJ-1 family members.[16a] To analyze the role of this residue for probe binding and catalysis, a point mutation was introduced by site-directed mutagenesis (Cys135Ala, C135A). Fluorescence SDS-PAGE analysis as well as mass spectrometry on the full-length proteins revealed, contrary to the wild type (wt) protein, a lack of **FM233** probe binding, suggesting an important role of Cys135 for SCRP-27A function (Figure 3B, left; see also Figures S15 and S16).

To narrow down its catalytic mechanism, we tested the enzymatic activity in various assays (see the Supporting Information for details). Interestingly, only the esterase assay with *para*-nitrophenyl acetate revealed slight turnover, which was abolished with the mutant and inhibited by **FM233** in a concentration-dependent manner (Figure S17). To then test the relevance of this putative esterase for bacterial viability, we constructed a non-polar deletion mutant of gene *yhbL* (STM3327) in *S.* Typhimurium LT2. Labeling of the 30 kDa protein was not observed in this mutant (Figure 3B, right), validating target binding and demonstrating that *yhbL* indeed encodes SCRP-27A. However, growth assays with **FM233** did not alter the MIC, indicating that this protein is not involved in the antibacterial mechanism of action.

GrxB and TrxA are well characterized enzymes that catalyze redox reactions of cysteine residues with crucial roles in related stress pathways.[13] They are important for reactivating oxidatively damaged proteins, and strains lacking thioredoxin and glutaredoxin oxidoreductases show impaired growth.[16] These mechanisms suggest that our compounds could mimic endogenous quinones and act as suicide inhibitors of TrxA and GrxB. We confirmed this notion by inhibition assays with both enzymes. TrxA as well as GrxB were inhibited in a concentration-dependent manner solely by **FM233** and, in line with the bioactivity data, not by the inactive control **FM375** (Figures 2E, S18, and S19).

Although we were not successful in determining the binding site by direct MS/MS sequencing owing to the poor ionization ability of the AEBQ moiety, MS analysis on the intact full-length protein confirmed irreversible modification of both enzymes (Figure S20). Moreover, **FM233** binding to GrxB and TrxA was further elucidated by molecular docking followed by molecular dynamics simulations and QM/MM calculations.[17] The surface representation of GrxB shows that **FM233** is buried in a deep pocket (Figure 4A) and stabilized by several hydrogen bonds (Figure 4B). In contrast, probe **FM375**, being devoid of the epoxide moiety, lacked the crucial contact to Lys129, resulting in 11 kcal mol^{-1} weaker interaction energy (Figure 4D and Table S4). A similar difference of 8 kcal mol^{-1} was observed for the binding of the active and inactive probes to TrxA (Figure 4F,H and Table S4). Here, the binding pocket is more surface-exposed with less stabilization, resulting in a 26 to 30 kcal mol^{-1} weaker interaction compared to GrxB (Figure 4E and

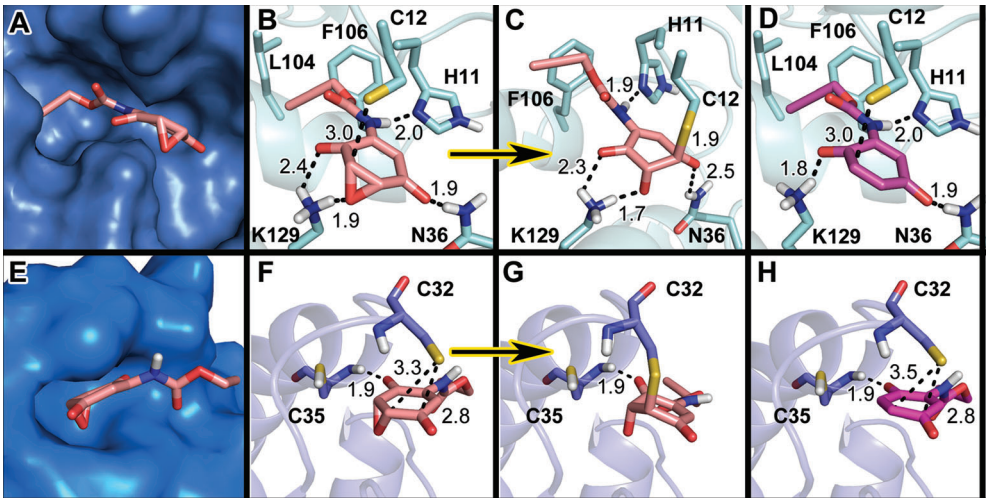

Figure 4. Conformation of the QM/MM-minimized structures of **FM233** within the receptors: GrxB (A: surface, B: ribbon) and TrxA (E: surface, F: ribbon). The covalently bound complexes of **FM233** to Cys12 and Cys32 within GrxB and TrxA are shown in (C) and (G), respectively. The QM/MM-minimized structures of the inactive control **FM375** within GrxB and TrxA are shown in (D) and (H). Only significant atoms are shown for clarity, all distances are given in Å.

Table S4). Based on the QM/MM-minimized structures, we modeled a possible reaction between **FM233** and the redox-active cysteine residues Cys12 and Cys32 of GrxB and TrxA, respectively. Both nucleophiles readily react with the electrophilic epoxide in an exothermal reaction (Figure 4C, G and Table S4). MD simulations performed for several docked complexes revealed fluctuations of the ligand positions within the binding site. This indicates that the partially surface-exposed location of the active sites enables diffusion of the ligands into the solvent. However, in the case of **FM233**, the covalent-bond formation, which is highly exothermic, keeps the probe within the protein, leading to stable inhibition.

With this mechanistic validation, we finally investigated the impact of **FM233** on oxidative stress in a cellular reactive oxygen species (ROS) assay (Figure 3C).[19] Interestingly, under ROS conditions, only active **FM233**, but not inactive **FM375**, induced a significant reduction in bacterial viability compared to the untreated control. The antibiotic activity of **FM233** thus stemmed to a large extent from the down-regulation of the enzymatic stress response and the corresponding sensitization of the cells to stress. In fact, quinones are known to trigger ROS production through the formation of semiquinone radicals. Moreover, quinone-mediated thiol S-alkylation results in the aggregation and depletion of thiol-containing proteins that are important for cellular homeostasis.[20]

In conclusion, AEHCs and AEBQs are privileged motifs of diverse natural products with fine-tuned reactivity towards nucleophilic residues. Profiling of these compounds against a panel of pathogenic bacteria revealed molecules with antibiotic activity even against challenging *S.* Typhimurium strains. A closer mechanistic inspection revealed that the simultaneous inhibition of two enzymes involved in oxidative stress response significantly impaired bacterial viability. Targeting GrxB and TrxA with natural-product-inspired quinone mimics thus represents an intriguing approach for the discovery of novel antibacterial compounds.

Acknowledgments

This work was funded by the Deutsche Forschungsgemeinschaft, SFB749, CIPSM, FOR1406, and Fonds der chemischen Industrie. We thank Prof. Michael Groll for access to the crystallization facility and Fabian Koczian for help with the FACS assay. Moreover, we are grateful to Astrid König, Katja Bäuml, and Mona Wolff for support.

Keywords: antibiotic resistance · covalent inhibitors · Gram-negative bacteria · stress response · quantitative proteomics

[1] a) J. M. Thomson, R. A. Bonomo, *Curr. Opin. Microbiol.* **2005**, *8*, 518–524; b) A. L. Meyer, *Curr. Opin. Pharmacol.* **2005**, *5*, 490–494.
[2] D. J. Payne, M. N. Gwynn, D. J. Holmes, D. L. Pompliano, *Nat. Rev. Drug Discovery* **2007**, *6*, 29–40.
[3] B. Swaminathan, P. Gerner-Smidt, T. Barrett, *Foodborne Pathog. Dis.* **2006**, *3*, 154–156.
[4] J. Marco-Contelles, M. T. Molina, S. Anjum, *Chem. Rev.* **2004**, *104*, 2857–2900.
[5] J. U. N. Kohno, M. Nishio, K. Kawano, N. Nakanishi, S.-I. Suzuki, T. Uchida, S. Komatsubara, *J. Antibiot.* **1996**, *49*, 1212–1220.
[6] a) V. V. Rostovtsev, L. G. Green, V. V. Fokin, K. B. Sharpless, *Angew. Chem. Int. Ed.* **2002**, *41*, 2596–2599; *Angew. Chem.*

2002, *114*, 2708 – 2711; b) C. W. Tornøe, C. Christensen, M. Meldal, *J. Org. Chem.* **2002**, *67*, 3057 – 3064.
[7] M. Hamada, Y. Niitsu, C. Hiraoka, I. Kozawa, T. Higashi, M. Shoji, K. Umezawa, T. Sugai, *Tetrahedron* **2010**, *66*, 7083 – 7087.
[8] R. Thiericke, A. Zeeck, A. Nakagawa, S. Omura, R. E. Herrold, S. T. S. Wu, J. M. Beale, H. G. Floss, *J. Am. Chem. Soc.* **1990**, *112*, 3979 – 3987.
[9] M. C. K. Leung, P. L. Williams, A. Benedetto, C. Au, K. J. Helmcke, M. Aschner, J. N. Meyer, *Toxicol. Sci.* **2008**, *106*, 5 – 28.
[10] I. Sattler, R. Thiericke, A. Zeeck, *Nat. Prod. Rep.* **1998**, *15*, 221 – 240.
[11] M. J. Evans, B. F. Cravatt, *Chem. Rev.* **2006**, *106*, 3279 – 3301.
[12] G. Liu, J. Zhou, Q. S. Fu, J. Wang, *J. Bacteriol.* **2009**, *191*, 6394 – 6400.
[13] W. A. Prinz, F. Åslund, A. Holmgren, J. Beckwith, *J. Biol. Chem.* **1997**, *272*, 15661 – 15667.
[14] A. Derouaux, B. Wolf, C. Fraipont, E. Breukink, M. Nguyen-Distèche, M. Terrak, *J. Bacteriol.* **2008**, *190*, 1831 – 1834.
[15] a) Y. Wei, D. Ringe, M. A. Wilson, M. J. Ondrechen, *PLoS Comput. Biol.* **2007**, *3*, e15; b) S.-J. Lee, S. J. Kim, I.-K. Kim, J. Ko, C.-S. Jeong, G.-H. Kim, C. Park, S.-O. Kang, P.-G. Suh, H.-S. Lee, S.-S. Cha, *J. Biol. Chem.* **2003**, *278*, 44552 – 44559.
[16] a) R. Ortenberg, S. Gon, A. Porat, J. Beckwith, *Proc. Natl. Acad. Sci. USA* **2004**, *101*, 7439 – 7444; b) C. Scharf, S. Riethdorf, H. Ernst, S. Engelmann, U. Völker, M. Hecker, *J. Bacteriol.* **1998**, *180*, 1869 – 1877.
[17] I. Antes, *Proteins Struct. Funct. Bioinf.* **2010**, *78*, 1084 – 1104.
[18] C. Jacob, A. L. Holme, F. H. Fry, *Org. Biomol. Chem.* **2004**, *2*, 1953 – 1956.
[19] S. Ahuja, L. Rouge, D. L. Swem, J. Sudhamsu, P. Wu, S. J. Russell, M. K. Alexander, C. Tam, M. Nishiyama, M. A. Starovasnik, C. M. Koth, *Structure* **2015**, *23*, 713 – 723.
[20] H. Antelmann, J. D. Helmann, *Antioxid. Redox Signaling* **2011**, *14*, 1049 – 1063.
[21] Structural coordinates and structure factors were deposited in the PDB database (http://www.ebi.ac.uk/pdbe/), accession code 5LIR.

Received: July 29, 2016
Published online: ■■ ■■, ■■■■

Communications

Drug Discovery

F. A. Mandl, V. C. Kirsch, I. Ugur, E. Kunold, J. Vomacka, C. Fetzer, S. Schneider, K. Richter, T. M. Fuchs, I. Antes,* S. A. Sieber* ____ ▮▮▮▮–▮▮▮▮

Natural-Product-Inspired Aminoepoxybenzoquinones Kill Members of the Gram-Negative Pathogen *Salmonella* by Attenuating Cellular Stress Response

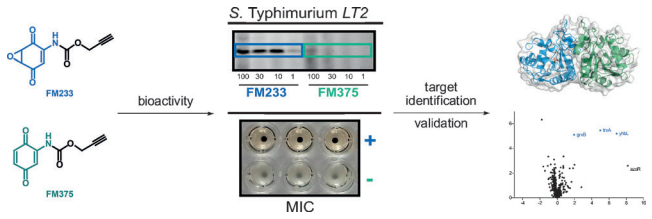

Aminoepoxycyclohexenones inhibit the growth of Gram-negative *Salmonella* in the low micromolar range. The bacterial targets of these antibiotics were analyzed by quantitative ABPP, which revealed a link to bacterial stress response that was validated by various assays. Aminoepoxybenzoquinones were thus validated as natural product scaffolds with suitable properties for the growth inhibition of *Salmonella*.